17.3 Testing of a new nonlocal boundary layer vertical diffusion scheme in numerical weather prediction applications

Song-You Hong

Laboratory for Atmospheric Modeling Research / Department of Atmospheric Sciences, Yonsei University, Seoul 120-749, Korea

Jimy Dudhia

Mesoscale and Microscale Meteorology Division/National Center for Atmospheric Research, Boulder, Colorado, USA

1. Introduction

The nonlocal boundary layer vertical diffusion scheme implemented by Hong and Pan (1996, HP hereafter) for the operational MRF model revealed a consistent improvement of the skill for precipitation forecasts over the continental US in the NCEP MRF model (Caplan et al. 1997). This scheme has been selected as the PBL scheme for the NCEP-DOE reanalysis II and contributed to a better water and energy budget in the reanalysis (Roads et al. 2002). Features of monsoonal precipitation and associated large-scale features over India were greatly improved compared with the results from a local approach (Basu et al 2002).

While the MRF scheme has extensively been evaluated in the NCEP operational models and MM5, some deficiencies have been reported. A typical problem lies in the fact that the scheme produces too much mixing. Mass et al. (2002) determined that the scheme produces too much mixing during a part of the day that results in excessive winds near the surface at night. Braun and Tao (2000) showed that in the simulation of hurricane Bob (1991) the MRF scheme produced the weakest storm among the PBL schemes in MM5, which is due to excessively deep vertical mixing drying the lower PBL. Bright and Mullen (2002) demonstrated that the MRFPBL scheme weakens the convective inhibition, which in turn provides a limiting factor in the model's ability to produce accurate quantitative precipitation forecasts during the southwestern monsoon over the US.

Recently, Noh et al. (2003, N2003 hereafter) proposed some modifications to the TM method based on large-eddy simulation data. Major modifications made by N2003 include: 1) an explicit treatment of the entrainment process of heat and momentum fluxes at the inversion layer, 2) vertically varying parameters in the PBL, and 3) the inclusion of the nonlocal mixing of momentum. N2003 revealed that the first factor is the most critical to the improvement, which resolves the problem of too strong mixing with strong wind shear and too little in the convection-dominated PBL.

Based on the study of Noh et al. (2003), and accumulated realization of the behavior of the Troen and Mahrt concept implemented by Hong and Pan (1996) for NCEP MRF and the NCAR MM5, a revised vertical diffusion algorithm that is suitable for weather forecasting and climate prediction models is developed after further generalization and reformulation.

The present paper documents some results in numerical weather prediction applications. A mesoscale convective system over Minnesota during 11-12 June 2001 is selected. A detailed description of the new scheme, together with the results for an idealized dry convection case, is available in our companion paper (Hong et al. 2003).

2. A review of the performance of the MRFPBL

As shown by HP, the determination of the boundary-layer height, *h,* is the most critical to the representation of nonlocal mixing. Following the derivation of Troen and Mahrt(1986), the boundary-layer height is given by

$$h = Rib_{cr} \frac{\theta_{va} |U(h)|^2}{g(\theta_v(h) - \theta_s)}, \quad (1)$$

where Rib_{cr} is the critical Bulk Richardson number, $U(h)$ is the horizontal wind speed at h, θ_{va} is the virtual potential temperature at the lowest model level, the $\theta_v(h)$ is the virtual potential temperature at *h*, and θ_s is the appropriate temperature near the surface. The temperature near the surface is defined as

$$\theta_s = \theta_{va} + \theta_T (= b\frac{\overline{(w'\theta_v')_0}}{w_s}), \qquad (2)$$

where θ_T is the scaled virtual temperature excess near the surface. W_s is the mixed layer velocity scale (= $u_* \phi_m^{-1}$) where u_* is the surface frictional velocity scale, and ϕ_m is the wind profile function evaluated at the top of the surface layer. $\overline{(w'\theta_v')_o}$ is the virtual heat flux from the surface and the proportionality factor, *b*, is set as 7.8.

Several factors and uncertainties lie in the determination of *h*. θ_T in (2) sometimes could become too large when the surface wind is very weak, resulting in unrealistically large *h* as pointed out by HP. For this reason, HP put a maximum limit of θ_T as 3 K. On the other hand, *h* could be too large when wind speed at a level z is too strong as shown by N002 and Mass et al. 2002. An apparent reason is due to the characteristics of the bulk Richardson number at a level z, that is given by,

$$Rib(z) = \frac{g(\theta_v(z) - \theta_s)z}{\theta_{va}U(z)^2} \qquad (3)$$

In eq 3, it can be seen that the thermal excess $(\theta_v(z) - \theta_s)$ due to the non-zero Rib_{cr} (=currently 0.5) becomes larger as wind speed at z is stronger since computed Rib is reduced when wind speed is weak. For example, the excess amount is as big as 3.4 K given that θ_{va} is 300 K, U(z) 15 ms-1, and the estimated pbl height, z, at 1000 m, which is not an unusual meteorological situation.

The excess can be as large as 6.1 K when wind speed is 20 ms-1. The combined effects of the thermal excess due to the surface flux in (2) and the Bulk Richardson number in (3) can be unrealistically large. This would explain too much mixing over the valleys in the western US (Manning et al. 2002). Furthermore, the eq. 3 provides information that the estimated Rib increases as z increases given the same temperature perturbation and wind speed, which implies more mixing when h is smaller. HP pointed out that there was too much mixing in the morning and noon.

Occasionally too much mixing has also been a problem since it was implemented into the NCEP MRF model in 1995. A smaller Rib_{cr} reduces the turbulent intensity by weakening the entrainment effect, which could sometimes provide a more realistic PBL structure, particularly when wind is strong and the boundary layer develops. However, based on the long-term evaluation of the scheme in the MRF model, the overall performance of the scheme for the forecast of precipitation was degraded when the entrainment was weakened, as demonstrated by HP.

3. A revised vertical diffusion package

For the mixed layer, following N2003, the turbulence diffusion equations for prognostic variables(*C; u, v,* θ, *q u v, qc, qi*) can be expressed by

$$\frac{\partial C}{\partial t} = \frac{\partial}{\partial z}\left(K_c \left(\frac{\partial C}{\partial z} - \gamma_c \right) - \overline{(w'c')_h} \left(\frac{z}{h} \right)^3 \right) \qquad (4)$$

where K_c is the eddy diffusivity coefficient and γ_c is a correction to the local gradient which incorporates the contribution of the large-scale eddies to the total flux. $\overline{(w'c')_h}$ is the flux at the inversion layer.

A major difference from TM is the explicit treatment of the entrainment processes through the 2nd term on the r.h.s. of (2), whereas the entrainment is implicitly parameterized by raising h above the minimum flux level. Above the mixed layer, the local diffusion approach is applied to account for free atmospheric diffusion. In the free atmosphere, the turbulent mixing length and stability formula based on observations (Kim and Mahrt 1992) are utilized.

The overall concept proposed by N2003 is adapted. In N2003, the moisture effect was neglected. Also, further generalization and reformulation of the proposed formula in N2003 is crucial. A comprehensive description of the new scheme focusing on the differences after HP is presented here. The numerical discretization of the scheme is a critical component due to the inclusion of the minimum heat flux in the r.h.s. of (4). A careful consideration was undertaken so as to ensure that the scheme works on a low vertical resolution grid, typical of mesoscale models.

a. Mixed layer diffusion

As in HP and TM, the momentum diffusivity coefficient is formulated as

$$K_m = kw_s z(1-\frac{z}{h})^p, \quad (5)$$

where p is the profile shape exponent taken to be 2, k is the von Karman constant (=0.4). z is the height from the surface and h is the height of the PBL. The mixed layer velocity scale of N2003 increases upward, rather than being a constant as in TM, which is represented as

$$w_s = (u_*^3 + \phi_m k w_{*b}^3 z/h)^{1/3}, \quad (6)$$

where u_* is the surface frictional velocity scale, and ϕ_m is the wind profile function evaluated at the top of the surface layer.

In order to satisfy the compatibility between the surface layer top and the bottom of the PBL, the identical profile functions to those in the surface layer physics are used. First, for the unstable and neutral conditions ($(\overline{w'\theta_v'})_o > 0$),

$$\phi_m = (1-16\frac{0.1h}{L})^{-1/4}, \text{ for } u \text{ and } v \quad (7)$$

$$\phi_t = (1-16\ \frac{0.1h}{L})^{-1/2}, \text{ for } \theta \text{ and } q$$

while for the stable regime ($(\overline{w'\theta_v'})_o < 0$),

$$\phi_m = \phi_t = (1+5\frac{0.1h}{L}), \quad (8)$$

where h is again the boundary-layer height, and L is the Monin-Obukhov length scale. The top of the surface layer is estimated as $0.1h$. In order to determine the b factor in (4), the exponent of -1/3 is chosen to ensure the free-convection limit. Therefore, we use the following approximation.

$$\phi_m = (1-16\frac{0.1h}{L})^{-1/4} \approx (1-8\frac{0.1h}{L})^{-1/3}, . \quad (9)$$

Following the N2003 and Moeng and Sullivan (1994), the heat flux amount at the inversion layer is expressed by

$$(\overline{w'\theta'})_h = -4.5 w_m^3 / h \quad (10)$$

where w_m is the entrainment velocity scale ($w_m^3 = w_*^3 + 5u_*^3$), and the mixed layer velocity scale for the dry air, $w_* = [(g/\theta_a)(\overline{w'\theta'_0})h)]^{1/3}$. Eq. (10) can be generalized for moist air with a non-dimensional constant, which can be expressed by

$$(\overline{w'\theta_v'})_h = -0.15\left(\frac{\theta_{va}}{g}\right) w_m^3 / h = -K_t(h)\frac{\partial \theta_v}{\partial z} \quad (11)$$

where w_m considers the moisture effect for buoyancy, and $K_t(h)$ the diffusion coefficient at the inversion layer.

As shown by N2003 and HP, the specification of the boundary layer height, h, is critical to the performance of the scheme. Note that in HP and TM the definition of the boundary layer height, h, is the level where the diffusivity becomes zero, whereas it is defined at the minimum heat flux level in N2003. In this study, h is determined to be the first neutral level from the lowest model level considering the temperature perturbation due to surface buoyancy flux, which can be expressed by,

$$\theta_v(h) = \theta_{va} + \theta_T \ (= a\frac{(\overline{w'\theta_v'})_0}{w_{s0}}) \quad (12)$$

where the $\theta_v(h)$ is the virtual potential temperature at *h.* The above θ_T formula is the same as that in HP, but the thermal excess term, θ_T, is smaller than that in the HP due to a larger ws0. θ_T ranges less than 1 K under clear sky conditions, whereas its maximum ranges up to 3 K in HP.

b. Free atmosphere diffusion

Above the inversion level (z=h), the local diffusion scheme, the so called “local-*K* approach” (Louis 1979), is utilized considering the depth for entrainment over *h.* N2003 assumes that fluxes decrease exponentially with z over the entrainment depth, δ. We can simply formulate the diffusion coefficients for momentum (*m; u,v*) and mass (*t; θ,q*), which are expressed by

$$K_{m,t} = K_{m,t}(h)\exp\left[-\frac{(z-h)^2}{\delta^2}\right] \quad (13)$$

where following N2003, the thickness of the entrainment zone can be estimated as

$$\delta / h = d_1 + d_2 w_m^{\ 2} / \Delta b \qquad (14)$$

where w_m is the velocity scale for the entrainment, $\Delta b = [(g/\theta_{va}) h \Delta\theta_v(h)]$ is the convective Richardson number, and d_1 and d_2 are constants, which are set as 0.02 and 0.05.

We also compute the vertical diffusivity coefficients for momentum (*m; u,v*) and mass (*t;* θ*,q*), following Louis et al. above *h,* represented by

$$K_{m,t} = l^2 f_{m,t}(Rig)\left|\frac{\partial U}{\partial z}\right| \qquad (15)$$

in terms of the mixing length, *l*, the stability functions, $f_{m,t}(Rig)$, and the vertical wind shear, $\left|\frac{\partial U}{\partial z}\right|$. The stability functions, $f_{m,t}$, are represented in terms of the local gradient Richardson number. For a non-cloudy layer, *Rig*= $g\ /T\ (\frac{\partial\theta_v\ /\partial z}{|\partial U\ /\partial z\,|^2})$). For cloudy air, Rig is modified by enhanced mixing due to clouds, which can be expressed by,

$$Rig_c = (1 + \frac{L_v q_v}{R_d T})[Rig - \frac{g^2}{|\partial v/\partial z|^2}\frac{1}{C_p T}\frac{(A-B)}{(1+A)}] \qquad (16)$$

where A = $\frac{L_v^{\ 2} q_v}{C_p R_v T^2}$ and B = $\frac{L_v q_v}{R_d T}$. The above formula is adapted from Durran and Klemp (1982), but with simplification. For cloudy air, Rig is replaced by Rig_c. The computed Rig is bounded to -100 to prevent unrealistically unstable regimes. The mixing length scale, *l*, is given by

$$\frac{1}{l} = \frac{1}{kz} + \frac{1}{\lambda_0} \qquad (17)$$

where *k* is the von Karman constant(=0.4), *z* is the height from the surface. λ_0 is the asymptotic length scale(=150 m), which is based on Kim and Mahrt (1992).

4. One-dimensional offline tests

The one-dimensional code is identical to the WRF module, but with a driver routine providing an idealized surface boundary forcing. Two sets of the experiments are designed. One is a high-resolution experiment with the number of vertical levels, 138, and the other, a low-resolution with 10 levels in the vertical. For both runs, the model top is located at 2750 m. The lowest model level is located at 10 m and equally spaced in the vertical with the interval of 20 m up to the model top, which is regarded to be a LES resolution. The low-resolution experimental setup has the lowest model level at 50 m, and 150, 300, 500, 750, 1050, 1400, 1800, 2250, and 2750 m, which is regarded to be a normal resolution for weather forecast models. The model integration time step is 1 sec and 5 min, respectively.

(a) (b)

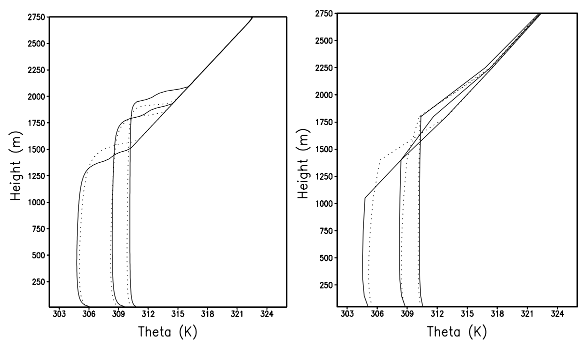

Fig. 1. The profiles of the potential temperature from the YSU (solid) and MRF (dotted) from the high resolution (138 level) (upper) and low resolution (10 level) (lower panel), at 11 AM, 2 PM and 5PM.

Figure 1 compares the profiles of the potential temperature from the two experiments. One can see that the YSUPBL scheme produces less mixing before noon, and more after 2 PM. More mixing in the morning by the MRFPBL is due to enhanced entrainment when wind is strong at the pbl top, which decreases the bulk Richardson number. Too strong mixing in the morning has been a typical problem in the NCEP MRF model. This was also pointed out by Hong and Pan from their evaluation of the performance with FIFE observations. A lower PBL height in the afternoon from the MRFPBL reflects the underestimation of the downward mixing under the situation of a purely convectively driven turbulence. N2003 and Ayotte et al. (1996) pointed out the behavior of the TM approach as a typical problem based on their evaluations with LES data sets. However, it is noticed that the problem in MRF does not appear in lower resolution grid. Indeed, there has not been a report about the systematic underestimation of turbulent mixing using the MRF scheme. The moisture profile underwent the same evolution as in the temperature (not shown).

5. A case study for a mesoscale convective system during 11-12 June 2001

During the late afternoon of 11 June 2001 a mesoscale convective system formed along the eastern border of the Dakotas. This system developed a prominent bow echo and produced a broad swath of wind damage as it propagated into Minnesota and raced southwestward across southern Wisconsin (Fig. 1). During its mature stage, radar images revealed a prominent high-reflectivity bow structure on its leading edge and a large region of moderately high reflectivity trailing to the north and northwest. The 24 hour accumulated precipitation showed precipitation

The WRF model was initialized at 1200 UTC 11 June 2001 with the initial and boundary data from the Eta analysis, which is a test dataset available at the WRF web site, and was run for 24 hrs. The model resolution is approximately 10 km.

It can be seen that the YSU scheme produced a more distinct inversion at 850 hPa level than the MRF scheme. This is due to the fact that the MRF scheme mixes the air too much. As a result, the CAPE is larger in the YSU experiment than in the MRF. The weak low-level inversion was reported to be a problem of the MRF PBL (Bright and Mullen 2002). It was found that the YSU scheme simulated warmer and drier profiles at 850 hPa than the MRF (not shown), which indicates a possibility of resolving a typical problem with the MRF scheme in MM5.

(a) (b)

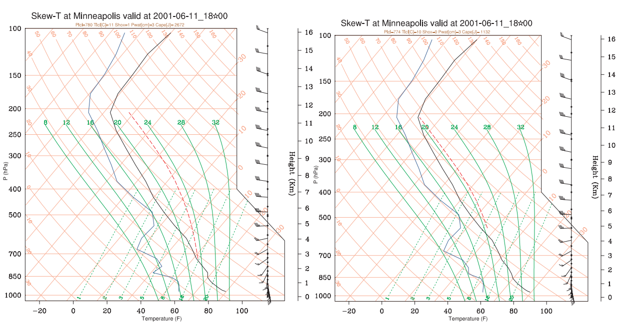

Fig. 2. Comparison of Skew-T log p thermodynamic profiles at 1800 UTC 11 June 2001 in Minneapolis , obtained from the experiments with (a) YSU and (b) MRF PBL schemes.

Figure 3 shows that the YSU scheme does not deteriorate in skill for the precipitation forecast. Both schemes simulated the precipitation distribution realistically in relation to the advance of the storm southeastward. The pressure distribution is also similar, but, interestingly, a bow type meso-high at the leading edge of the storm was better organized when the YSU scheme is used.

(a) (b)

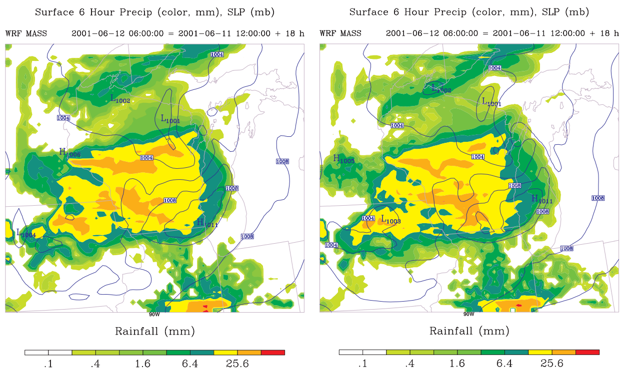

Fig. 3. Comparison of 6-hr accumulated precipitation (mm; shaded) and sea level pressure (hPa; solid lines) valid at 0600 UTC 12 June 2001, obtained from the experiments with (a) YSU and (b) MRF PBL schemes.

6. Concluding remarks

The new scheme has shown the major benefit of a realistic evolution of the mixed layer height. The new scheme is found to be able to outperform the MRF pbl scheme for selected cases of severe weather. For a localized convection over US, the new scheme has a capability of resolving meso-highs and the gust front very well.

The new scheme has been tested in a daily forecast framework at NCAR (http://rain.mmm.ucar.edu /mm5/pages/wrf.html). Based on the detailed evaluation of the results, the scheme has been reformulated to work better in GCM as well as NWP model. It is scheduled to be released to the public in WRF Version 2 around the end of 2003.

7. Acknowledgments

This study is supported by the Ministry of Science and Technology through National Research Laboratory Program, and by the KMA through the R&D project. The first author thanks NCAR for providing working facilities as a visiting scientist in the 2002 and 2003 summers.

8. References

Ayotte, and co-authors, 1995 : An evaluation of neutral and convectively planetary boundary layer parameterizations relative to large eddy simulations. *Bound.-Layer Meteor*., 79, 131-175.

Caplan, P., J. Derber, W. Gemmill, S.-Y. Hong, H.-L. Pan, and D. Parrish, 1997: Changes to the 1995 NCEP operational medium-range forecast model analysis-forecast system. Wea. and Forecasting, 12, 581-594.

Basu, Swati, G. R. Iyengar, A. K. Mitra, 2002: Impact of a Nonlocal Closure Scheme in a Simulation of a Monsoon System over India. Mon. Wea. Rev., 130, 161–170.

Bright, David R., Steven L. Mullen, 2002: The Sensitivity of the Numerical Simulation of the Southwest Monsoon Boundary Layer to the Choice of PBL Turbulence Parameterization in MM5. *Wea. and Forecasting*, 17, 99–114.

Braun, Scott A., Wei-Kuo Tao, 2000: Sensitivity of high-Resolution Simulations of Hurricane Bob (1991) to Planetary Boundary Layer Parameterizations. *Monthly Weather Review*: Vol. 128, No. 12, pp. 3941–3961.

Chen, S.-H., and J. Dudhia, 2000: Annual report: WRF physics [Available from http://wrf-model.org],

Hong, S.-Y., H.-L. Pan, 1996 : Nonlocal boundary layer vertical diffusion in a Medium-Range Forecast model. Mon. Wea. Rev., 124, 2322-2339.

Hong, S.-Y., Y. Noh, and J. Dudhia, 2003: A new vertical diffusion package with explicit treatment of the entrainment processes. Part I: Formulation and one-dimensional tests. In preparation.

Noh, Y., W.G. Cheon, S.-Y. Hong, and S. Raasch, 2003: Improvement of the K-profile model for the planetary boundary layer based on large eddy simulation data. Bound.-layer Meteor., 107, 401-427.

Persson, P., B. Walter, J-W bao, and S. Michelson, 2001: Validation of boundary-layer parameterizations in maritime storm using aircraft data. The ninth conference on mesoscale processes, Ft. Lauderdale, FL, July30-Aug. 2.

Roads, J., Kanamitsu M., and R. Stewart, 2002: CSE water and energy budgets in the NCEP-DOE reanalysis II. J. Hydrometeor., 3, 227-248.

Stevens, B., 2000: Quasi-Steady Analysis of a PBL Model with an Eddy-Diffusivity Profile and Nonlocal Fluxes. *Monthly Weather Review*: Vol. 128, No. 3, pp. 824–836.

Troen, I., and L. Mahrt, 1986: A simple model of the atmospheric boundary layer; Sensitivity to surface evaporation. *Bound.-Layer Meteor*., 37, 129-148.

Mass, C. F., D. Ovens, K. Westrick, and B.A. Colle, 2002: Does increasing horizontal resolution produce more skilful forecasts ? Bull. Amer. Meteor. Soc., 407-430.

Farfán, L. M., and J. A. Zehnder, 2001 : An Analysis of the Landfall of Hurricane Nora (1997), Mon. Wea. Rev.,, 129, 2073–2088.